GEOFIZIKA VOL. 42 2025

DOI: https://doi.org/10.15233/gfz.2025.42.3
Original scientific paper

A brief analysis of the supercell storm in Croatia on 19 July 2023

Nebojša Subanović [1], *Ivan Toman* [2], *Patrik Jureša* [3] *and Branko Grisogono* [3]

[1] Power Net simple Ltd., Zagreb, Croatia

[2] Maritime Department, University of Zadar, Zadar, Croatia

[3] Department of Geophysics, Faculty of Science, University of Zagreb, Zagreb, Croatia

Received 24 June 2024, in final form 19 December 2024

Supercell storms, or super-Cb, are powerful and long-lasting convective systems that can form within statically unstable air mass in favourable dynamic conditions. These severe storm types are characterized by one or more rotation updrafts, usually supported by environmental vertical wind shear. Severity of these systems is usually reflected in heavy precipitation, large hail, hurricane wind gusts and sometimes derecho or tornado events.

On 19 July 2023, a supercell thunderstorm impacted Croatia, including the capital, Zagreb. It originated in the western Po River valley, Italy, progressed over Slovenia, Croatia, and finally dissipated over Serbia. Its track crossed about 1000 km long path and lasted approximately 9 h, leading to human casualties and heavy property damages.

The synoptic and mesoscale conditions leading to the formation of the supercell is analysed and discussed. Regular official station data, synoptic charts, upper air soundings, radar, and satellite observations are deployed as well as WRF model simulation performed for this case scenario. This study contributes to better understanding of such phenomena and their destructive potential in the broader region of Croatia and adds to somewhat scarce research field of such weather in this part of the world.

Keywords: mesofront, severe convective storms, derecho, bow echo

1. Introduction

Using the European Severe Weather Database (ESWD), a comprehensive repository of severe weather events and their associated data across Europe, Pacey et al. (2021) analysed cases between 2009 and 2018 and found that severe

convective wind days have increased from 50 days per year in 2009 to 117 days per year in 2018, largely because of an increase in reporting. Nevertheless, many statistical data show an actual increase in frequency of convective storms occurrence over European countries. We found for the Zagreb Maksimir station (Croatia) that between 2000 and 2023, an average of 14 convective storms per year were recorded while 2023 shows an increase to 31 such event. Most of the convective storms occur between May and September, averaging 12 per year for this area and period. The most of such storms can be classified as a single or multicellular type (Strelec Mahović et al., 2007).

Supercells or super-Cb are very powerful and long-lasting convective storm systems that form within statically unstable atmospheric conditions. Contrary to the non-supercell storm type, they are characterized by rotating updraft, sometimes even a few of them (see below), which combined with vertical wind shear allow that their lifetime may extend beyond 4-5 h (*e.g.* Bunkers et al., 2006).

The main characteristics of supercells include:

1. Self-developed rotating updraft: This is a vertical column of moist and warm air that rotates around its axis. This rotation contributes to the longevity of the storm and can potentially generate very strong smaller scale vortices such as tornadoes (Klemp, 1987).

2. Intensity: These storms typically bring strong winds, heavy rainfall, hail, and can produce very damaging features like tornadoes, downbursts and derechoes.

3. Longevity: non-supercell systems are usually short-lived, ~ 1–2 h, while supercell may last for several hours, though frontal non-supercell system can be long-living.

Supercells are well-described in numerous studies and have been modelled as well (*e.g.*, Orf et al., 2017). Although there are still some uncertainties, the main mechanism of their development and evolution is well understood. Supercells can exist independently or organize themselves into larger clusters. Apart from the mentioned updraft rotation, their complex internal structure enables continuous propagation, thus allowing them to persist for extended periods, unlike non-supercell systems which feature their average lifespan ~ 1 h. Moreover, on Doppler radar images, supercells' velocity fields often exhibit a distinctive hook shape.

The development of supercells and their rotation requires the presence of wind shear in the surrounding environment. Vertical wind shear separates updraft and downdraft columns, preventing downdrafts from interfering with the buoyant updrafts, and enhances entrainment and detrainment processes. Directional wind shear initiates horizontal vorticity, which, when tilted and stretched by updrafts, produces rotation around a vertical axis (*e.g.*, Strelec Mahović, 2007). This often leads to the splitting of the ascending column into two distinct, counter-rotating updrafts, with intense downdrafts and heavy precipitation occurring

between them. This separation forms two storm cells: left- and right-moving ones relative to the mean tropospheric wind. Additionally, the interaction of strong vertical wind shear with horizontal gradients of vertical velocity can also contribute to updraft rotation (*e.g.*, Holton, 1992), further enhancing storm organization and longevity.

Orography can have strong influence on the development of supercells by altering the regional wind regime, including increasing shear and forcing updrafts. Mountain ranges, by channelling surface winds, may accelerate the wind speed and thus create stronger shear. In addition, they can enhance convection on windward slopes and the related turbulence and shear on leeward slopes. Such significant effects usually enhance storm rotation and increase the likelihood of supercell formation. Smith et al. (2016a) in their study employ numerical simulations to examine how bell-shaped mountains of varying heights impact tornadic supercells. Their findings indicate that terrain-induced blocking effects can be dominant, causing shifts in storm tracks and enhancing inflow, which leads to increased precipitation, and it influences overall storm intensity.

Smith and Lin (2016) examined the influence of elongated, bell-shaped terrain on the development of supercell thunderstorms using numerical simulations with the Bryan Cloud Model 1. The experiments tested various configurations, including mountain heights of 500 m, 1000 m, and 1500 m, as well as different orientations of the terrain relative to the wind direction. The findings revealed that orography significantly affects the intensity and structure of supercells by modifying airflow, enhancing rotation, and influencing precipitation patterns. Greater airflow directed into the storms increases rainfall rates and cold pool depths, occasionally initiating additional convective processes. The simulations also demonstrated that tornadogenesis potential is enhanced under specific terrain configurations, while terrain blocking alone is insufficient to produce tornadoes. The most favourable configuration involved orienting the terrain to maximize vorticity is along the gust front. Their results highlighted the critical role of terrain in modulating supercell lifecycle and intensity, offering valuable insights for understanding and predicting supercell thunderstorms in complex orographic environments.

Contrasts between sea and land surfaces in coastal areas (Sano, 2006) create local instabilities, especially when moist sea air moves inland. These contrasts are often most pronounced during the day in warmer part of year, which can result in the development of convergence zones such as sea breeze fronts. Significantly, these boundaries can trigger convection and, in interaction with the surrounding atmosphere, lead to the formation and strengthening of supercells. Surface friction may increase boundary layer convergence and tilt horizontal eddies into vertical ones, thereby supporting the rotation. Furthermore, coastal uplift, variations in sea surface temperature, and interactions between sea breeze fronts and larger mesoscale boundaries usually produce additional effects on intensifying and accelerating the formation of storm systems.

The supercell events in Croatia have not been studied extensively yet, although some studies discussed few cases in Croatia and nearby regions. Stiperski (2005) analysed a tornadic supercell on 30 August 2003, identifying a baroclinic boundary in the northwestern Croatia as the main mesoscale feature during the storm. A baroclinic boundary is a region where isotherms and isobars intersect, leading to strong horizontal temperature gradients and the generation of atmospheric instability. Such boundaries are key zones for cyclogenesis, as they enhance the development of synoptic-scale disturbances through baroclinic instability and associated vertical wind shear. Furthermore, the supercell that featured a derecho-like event in Bulgaria on 20 July 2011 was analysed by Gospodinov et al. (2011). Similar case study analyses that often include numerical simulation of the related supercell, derecho or alike convective events have been performed for various cases over other parts of Europe (*e.g.*, Taszarek et al., 2019a; Ricci et al., 2020; Giovannini et al., 2021; Gatzen, 2004; Squitieri et al., 2023; Weisman et al., 2013).

The related climatological studies reveal that multiannual trends over most of Europe show an increase of severe convective weather frequency (*e.g.*, Taszarek et al., 2019b; 2021) with a projected further increase toward the end of the century due to expected enhancements of instability and low-level moisture content (Pučik et al., 2017). Such expected scenario warns for a better understanding of severe convective storms and their current and future potential in this part of Europe.

Ducrocq et al. (2014) described the HyMeX Special Observation Period 1 (SOP1), a field campaign focused on heavy precipitation events (HPEs) and flash flooding in the northwestern Mediterranean region. The Mediterranean's unique geography and orography, with steep coastal mountains and its role as a major source of heat and moisture, create conditions conducive to extreme precipitation and flooding. HPEs often arise from quasi-stationary mesoscale convective systems (MCSs) fuelled by warm, moist marine air and intensified by orographic lifting and baroclinic processes. The SOP1 campaign aimed to address key gaps in understanding by collecting extensive atmospheric, oceanic, and hydrological observations. It utilized advanced ground-based instruments, aircraft, and ocean profiling systems across multiple sites in France, Spain, and Italy. These observations provided critical insights into moisture sources, air-sea interactions, and the microphysics of MCSs, as well as the hydrological processes driving flash floods. Initial results emphasized the importance of mesoscale dynamics, orographic effects, and moisture transport in shaping these high-impact weather events. The findings offered a foundation for improving numerical weather prediction (NWP) models and highlight the value of interdisciplinary observation campaigns in understanding and mitigating the risks of severe weather in complex topographic regions.

Davolio et al. (2014) investigated a severe flash flood that occurred near Venice on 26 September 2007, during the MAP D-PHASE Operational Period.

A mesoscale convective system (MCS) formed in the convergence zone between a south-easterly low-level jet over the Adriatic Sea and a north-easterly barrier wind south of the Alps. This system produced over 320 mm of rainfall within 12 h, with 240 mm falling in just 3 h. High-resolution convection-resolving models, including MOLOCH, WRF, and MM5, were used to simulate the event and evaluate its predictability. The simulations revealed strong sensitivity to initial and boundary conditions, as well as to the model parameterization schemes, underscoring the challenges of forecasting convective rainfall. However, the large-scale environment, including the synoptic-scale flow and orographic effects, played a significant role in organizing the convection and enabling relatively accurate predictions with sufficient lead time. Orographic forcing contributed to the lee cyclogenesis, enhancing low-level flow convergence that sustained the MCS. These findings highlighted the importance of high-resolution modelling and the interplay of synoptic-scale dynamics and mesoscale processes, particularly in complex orographic regions, for understanding and predicting extreme weather events like flash floods.

Ricchi et al. (2023) investigated the extreme hailstorm that struck the Adriatic coastline on 10 July 2019, producing hailstones up to 14 cm in diameter near Pescara. Using high-resolution WRF model simulations with a 1 km grid spacing, the authors examined the role of sea surface temperature (SST) anomalies and orography in triggering and sustaining the supercell. The event was driven by a cold front interacting with warm, moist air over the Adriatic Sea and the Apennine orography. The findings highlight that positive SST anomalies (+2.7 °C basin-wide, peaking at +4.4 °C locally) enhanced surface heat fluxes, fuelling instability and supporting strong convection. Orography played a dual role by blocking the low-level cold air (Bora wind) and enhancing vertical wind shear along the coastline, facilitating supercell development. Sensitivity experiments revealed that modifying topographic features or removing SST anomalies significantly altered the storm's intensity, trajectory, and hail production. These results underscore the critical interplay between atmospheric dynamics, sea surface conditions, and complex orography in shaping severe weather events in the Mediterranean.

Tiesi et al. (2022) examined the giant-hail-producing supercell that struck Pescara, Italy, on 10 July 2019, generating hailstones with diameters up to 14 cm. Using high-resolution numerical simulations with the WRF model, the research analysed the synoptic and mesoscale conditions responsible for the storm's development. The interaction between the cold Bora wind descending from the Dinaric Alps and the warm, moist air over the Adriatic Sea resulted in strong vertical wind shear, which removed convective inhibition and enabled mesocyclonic rotation. The simulations showed that the Bora wind uplifted the unstable pre-existing air, triggering convection, while upper-level south-westerly winds enhanced shear and organized the supercell. The WRF-HAILCAST module accurately modelled hailstone characteristics, including size and distribution,

aligning well with radar observations and local reports. Sensitivity experiments revealed that the timing and accuracy of the simulations depended heavily on the initial and boundary conditions, with the best results achieved using the GFS analysis initialized 36 h before the event. These findings underscore the importance of high-resolution modelling, accurate initial conditions, and specialized hail modules for understanding and predicting extreme weather events like giant hailstorms, particularly in regions with complex orography such as the Mediterranean basin.

In this paper we present a case study of a severe supercell storm with an associated derecho event that crossed over the north-western, central, and eastern Croatia on 19 July 2023. The destruction was so extensive that four fatalities were recorded, around 20,000 structures were damaged, and, for emergency repairs to residential buildings, the government approved a €20 million aid package. Maximum wind speeds at the official weather stations of the Croatian Meteorological and Hydrological Service (DHMZ) ranged between 92 and 180 km/h (the latter was recorded at Gradište site, the eastern Croatia, where the instrument broke down together with parts of the site; thus, the true wind speed maximum remains unknown). Furthermore, this supercell brought in a new Croatian hail size record is 13 cm in diameter.

The aim of this study is to describe the meteorological situation and explain the mechanisms that led to the occurrence of supercell which ravaged the north-western, central, and eastern parts of Croatia. Such events are inadequately represented in scientific literature, and this work will, to a certain extent, fill the existing gap and contribute to improving the understanding and eventually prediction of these phenomena in the broader area of Croatia.

2. Methods

For the analysis of the synoptic situation that resulted in the onset, formation and further development of the supercell, we utilized measured and observed data, as well as results from simulations using WRF-ARW numerical model (Skamarock, W. C. et al., 2021). The vertical atmospheric structure was obtained from radiosonde observations from meteorological stations in Zagreb (Croatia), Novara, and Capofiume (Italy), which were retrieved from: https://weather.uwyo.edu/upperair/sounding.html.

Information about the height of the supercell, its speed, the lowest and mean cloud top temperatures, and the duration from the occurrence to arrival over Zagreb were sourced from the EUMETSAT website (EUMETSAT, n.d.). This service provides information on clouds related to significant convective systems, ranging from mesoscale (in this case, say, 200 to 2,000 km) to smaller scales (tens of km). A detailed description of the algorithms can be found in the Algorithm Theoretical Basis Documents (ATBD) (EUMETSAT, 2021a) and the Product

User Manual (UM, EUMETSAT, 2021b) of the EUMETSAT Nowcasting and Very Short-Range Forecasting software package for convective products.

We obtained radar images of reflectivity and precipitation from the Croatian Meteorological and Hydrological Service (DHMZ). Radar images of precipitation from the Slovenian radars were acquired from the website of the Environmental Agency of the Republic of Slovenia (https://www.arso.gov.si/). Synoptic charts were obtained from the website of the Deutscher Wetterdienst (https://www.dwd.de/).

The Weather Research and Forecasting (WRF) model, version 4.2.2, was used to simulate mesoscale and convective-scale atmospheric processes using a nested domain configuration. Three nested domains were configured with horizontal grid of 9 km, 3 km, and 1 km, (Fig. 1) and each domain consisted of 45 vertical levels. The parent domain (D01) comprised 114 × 86 grid points, while the nested domains (D02 and D03) refined the grid to 121 × 115 and 154 × 133 grid points, respectively. A 3:1 nesting ratio was applied between each domain to ensure smooth interaction within atmospheric dynamics. The simulation covered the period from 18 July 2023 at 00:00 UTC to 20 July 2023 at 00:00 UTC, with a time step of 50 s for the parent domain and a corresponding parent-to-nest time step ratio of 3:1. To improve numerical stability, vertical velocity damping was applied above 5,000 m. The first 24 h of the simulation were used for model spin-up and were excluded from the analysis. The vertical structure of the atmosphere was resolved using a hybrid vertical coordinate system, with the model top set at a pressure level of 50 hPa. Surface albedo values and leaf area index are included from MODIS static dataset. Cloud effects of cumulus parametrization scheme are included in the calculation of radiation fluxes.

The physical parameterizations used in the simulation included the Kain-Fritsch cumulus scheme for deep convection (active only in D01), WSM 6-class microphysics for cloud processes, the YSU planetary boundary layer scheme for turbulence, and the Noah Land Surface Model (LSM) for surface fluxes and energy balance. Radiation processes were represented by the RRTM longwave and Dudhia shortwave schemes, with a radiation time step of 1 minute. Land use was derived from the 21-category fluxes and energy balance. Radiation processes were represented by the RRTM longwave and Dudhia shortwave schemes, with a radiation time step of 1 minute. Land use was derived from the 21-category MODIFIED_IGBP_MODIS_NOAH dataset. Initial and boundary conditions were specified using external meteorological datasets, updated at 1 h intervals. Boundary conditions for the parent domain included a 5-grid-point buffer zone, while feedback between domains was disabled. Model output was generated hourly for the parent domain and every 30 minutes for the nested domains.

Dynamic options included a third-order Runge-Kutta integration scheme in time, fifth-order advection for horizontal momentum and scalars, and a sixth-order diffusion scheme with a diffusion factor of 0.12 to control numerical noise.

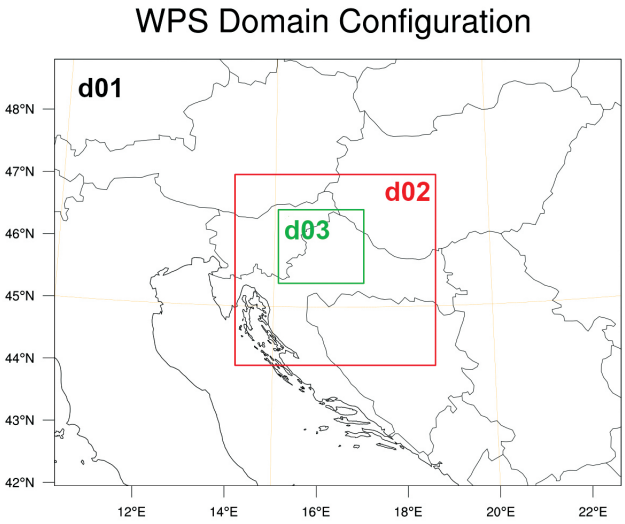

Figure 1. WRF Preprocessing System (WPS) spatial coverage of WRF model domains for simulation and analysis of the supercell storm, *i.e.*, supercell, in Croatia on 19 July 2023.

This configuration was designed to facilitate high-resolution modelling of atmospheric phenomena influenced by complex topography, land-sea interactions, and mesoscale dynamics. The combination of the WSM 6-class microphysics, the Kain-Fritsch cumulus parameterization, and YSU planetary boundary layer scheme showed satisfactory for the study objectives, balancing model accuracy, computational efficiency, and timeliness in investigating severe weather associated with deep moist convection.

The height above the ground of the first vertical level was 50 m as WRF default value. For the sea surface temperature (SST) we used the skin temperature, *i.e.*, skintemp variable from GFS.

3. Results

3.1. Description of the synoptic situation that preceded the event

Five to six days before the analysed event, a large extratropical cyclone formed over northwestern Europe with its centre west of Ireland. Deepening, its centre moved over Ireland and Scotland towards the northern Scandinavian Peninsula in the following days. At the same time, eastern and southeastern Europe has been under influence of the broad but weak anticyclone. This combination of pressure systems allowed for the influx of moist and somewhat cooler air from the North Atlantic, resulting in cloudy weather with precipitation over central Europe

and mostly clear and dry weather over eastern and southeastern parts of the continent. The highest daily temperatures in northern Italy, Slovenia, and Croatia ranged from 30 to 36 °C. The influx of moist and unstable air around the eastern Alps into southern and southeastern Europe initiated the formation of isolated Cb storm clouds. This situation remained until the analysed event.

The prolonged anticyclone provided favourable conditions for a consistent heating of southeast Europe and the accumulation of a large amount of thermal energy. The high dew point temperatures ranging from 22 to 26 °C contributed to latent heat accumulation. Finally, during the night from 18 July to 19 July, a substantial amount of cooler and unstable air, bypassing the Alps from the western side, crossed over the Po Valley. Similar synoptic pattern in the area has already been discussed in several papers (*e.g.* Alberoni et al., 1996; Feldman et al., 2004). At altitudes ranging from 1.5 km to 16 km, powerful winds from the west were estimated from radio soundings to exceed speeds of 25 m/s and more. Below 1.5 km, the wind was weak and variable, with speeds less than 3 to 5 m/s, indicating significant vertical wind shear.

According to radiosonde measurements from Novara Cameri station, Surface-based Convective Available Potential Energy (SBCAPE) increased from 2,450 at 00 UTC up to 4,600 J/kg at 12 UTC, 19 July. The Zagreb sounding at 12 UTC showed SBCAPE value of 1,680 J/kg (see later). Soundings from both stations indicate very strong wind shear around altitudes of 2,000 m (Novara) and 3,000 m (Zagreb). These parameters are indicative for strong convective intensity potential, and they also suggest vigorous forms of convection. The most likely triggering mechanism for this deep convection was when *"subtle upper-level vorticity maximum moved into the Po Valley, setting the stage for convective initiation of this volatile environment*" (https://www.estofex.org/cgi-bin/polygon/showforecast.cgi?text=yes&fcstfile=2023072006_202307182228_3_stormforecast.xml).

3.2. A brief chronological description of the event

During the morning of 19 July, in the northeast of Italy, deep convective clouds developed and progressed towards Slovenia. At 13 UTC, the storm system was in Slovenia, near the Croatian border. On the Slovenian precipitation radar image, Fig. 2, mesoscale cyclonic rotation is visible. At 13:30 h the storm system reached the Croatian border, undoubtedly forming a supercell. The rotation was pronounced, and the precipitation area had the shape of an inverted letter S. At 14 UTC, the supercell stretched from the town of Karlovac (Croatia) through Zagreb and Maribor (Slovenia), with its separation occurring above Zagreb. In this event tornadoes were not officially recorded, nor are there any other pieces of evidence of their occurrence, even though the destruction was of the same intensity as during tornado activity *e.g.*, (Pilguj, 2022). The propagation speed of the supercell above Slovenia and Croatia ranged from 60 to 80 km/h.

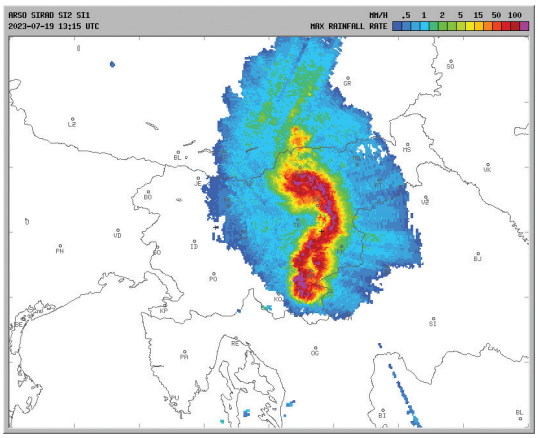

Figure 2. Rainfall rate radar image from the Slovenian radars. Precipitation field shows inverted "S shape". Image credit: ARSO website. The supercell approaches northwest of Croatia. Cities and towns are indicated.

The dimensions of the damage axis length, non-randomness of the path of occurrence along a singular swath, the number of damage reports and measured wind gusts as well as their temporal distribution, all fit well within the criteria for derecho event classification, established by Johns and Hirt (1987).

3.3. Analysis of radiosonde measurements

The dimensions of the damage axis length, non-randomness of the path of occurrence along a singular swath, the number of damage reports and measured wind gusts as well as their temporal distribution, all fit well within the criteria for derecho event classification, established by Johns and Hirt (1987).

Radiosonde data from Novara airport sounding, Fig. 3, clearly indicate that during the night of July 18–19, a large amount of SBCAPE accumulated in the northeast Italy region. The SBCAPE ranged between 1000 and 2500 J/kg with very low Surface-based Convective Inhibition (SBCIN) values.

Additionally, the bulk wind shear between 2000 and 2500 m of approximately 10–15 m/s was present within the area. Novara, Fig. 3, sounding distinctly shows high SBCAPE during the night, while the 00 UTC 19 July sounding, Zagreb, still indicates a defiance of instability caused by the latent heat shown below in Fig. 4. The 12 UTC 19 July soundings at all stations considered show large SBCAPE area on thermodynamic diagrams ≈ 2.5 km above ground level (AGL). Such a combination of wind shear and SBCAPE is optimal for the formation and propagation of supercells (*e.g.*, Holton, 1992). The Novara soundings at 12 UTC showed SBCAPE of 4,600 J/kg while Zagreb sounding measured 1,680 J/kg.

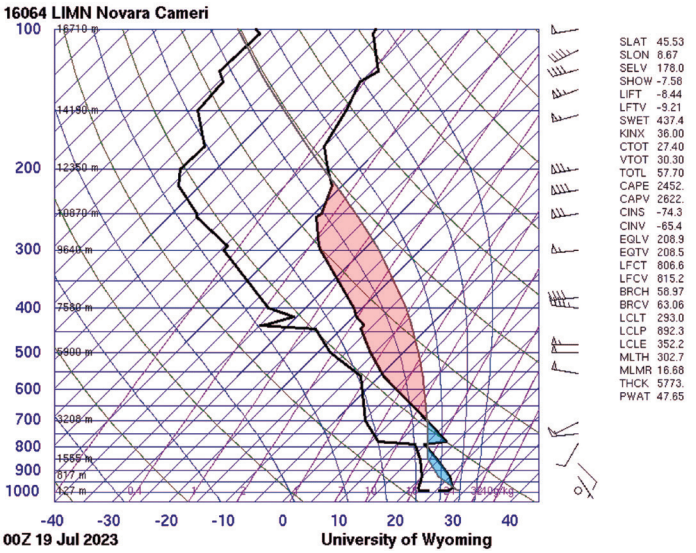

Figure 3. Skew-T log-P of Novara airport sounding at 00 UTC 19 July 2023. Novara airport (45.45° N 8.62° E) is about 50 km west from the centre of the city of Milano, Italy. Left black curve is dew point while right one is temperature. Transparent red area represents CAPE while blue area represents CIN. Image credit: University of Wyoming, USA.

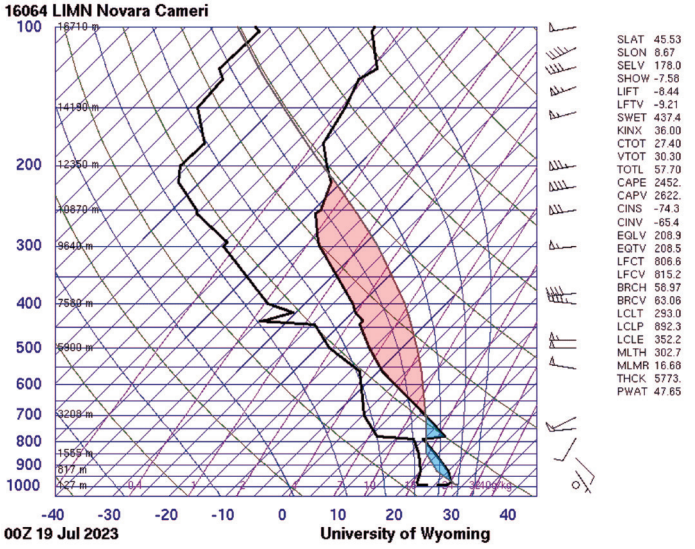

Figure 4. Skew-T log-P of Zagreb Maksimir station (45.82° N 16.03° E) sounding at 12 UTC 19 July 2023. Left black curve is dew point while right one is temperature. Transparent red area represents CAPE while blue area represents CIN. Image credit: University of Wyoming, USA.

The SBCAPE "area" in the Novara sounding plot at 00 and 12 UTC is quite "bulging," indicating a high likelihood of strong convection development (Holton, 1992; Klemp, 1987; Gregorič et al., 2003; Orf et al., 2017; Pacey et al., 2021). SBCIN area is positioned at quite high altitude. The 12 UTC sounding from Zagreb, Fig. 4, conducted 2 h before the arrival of the supercell over Zagreb, already shows a large but "thin" shape of SBCAPE area in sounding graphs and a wide SBCIN shape.

3.4. Analysis of radar and satellite images

EUMETSAT satellite imagery (not presented) indicates that the origin of the supercell was above the western end of the Po River valley. Progressing down the valley, the system intensified, and mesoscale cyclonic rotation initiated. Upon reaching Slovenia, the convective system exhibits structural and intensity features of a supercell. Moreover, at the time when the system was over Slovenia, several new smaller convective cells started to form on the southern slopes of the Alps and progressed towards the interior of Slovenia. Along the way they merged into two cells. The observed supercell crossed over Zagreb around 14 UTC, shown below in Fig. 5a, and continued towards Serbia where it dissipated.

Next, we analyse the chronological development of the storm based on precipitation and reflective radar images, using radar recordings from the Croatian Meteorological and Hydrological Service (DHMZ) and the Slovenian Environment Agency (ARSO). Bilogora radar (elevation 259 m ASL) reflectivity image captured at 13 UTC (not presented) shows the well-developed storm system over Slovenian-Croatian border. In Fig. 5a, the cyclonic rotation of the system is presented with "S" shape of the cloud top, resembling a typical mesocyclone with the band of heavy precipitation outlining its cold front, while Fig. 5b shows supercell timeline progression. This "S" shape is more clearly visible in the radar reflectivity image, Fig. 6. The propagation of the system takes south-eastern direction toward Zagreb with a rather high speed of about 70–80 km/h. According to the EUMETSAT data, when the supercell was over Zagreb, its top temperature was between –62 and –67 °C. By 14 UTC, the precipitation area clearly outlines the frontal zone and the rear of the storm. Radar reflectivity image from Bilogora radar station, Fig. 6, shows more than one cell, but from the image it is not very clear how many of them were present during the progression over Zagreb.

3.5. Simulation with WRF ARW numerical model

For a better understanding of the mechanisms that led to the formation of the supercell and its progression over Slovenia and northern Croatia, we conducted simulations using the numerical model WRF-ARW (Skamarock et al., 2021). The results of the numerical simulation are presented in the form of

near-surface and upper-level fields, skew-T log-P diagrams, and meteograms. Surface and upper-level field charts were used to give insights into the areas of precipitation, horizontal distribution of temperature, and wind vectors. Skew-T

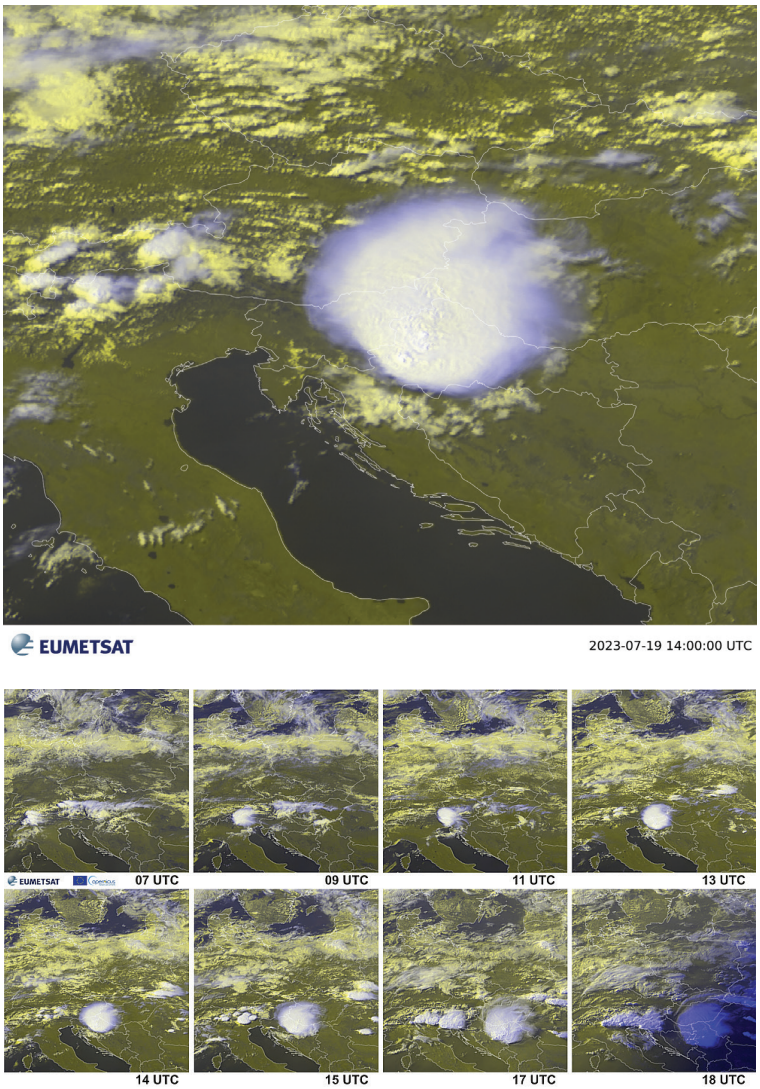

Figure 5. *a*) EUMETSAT European HRV RGB (High Resolution Visible Red, Green, and Blue) satellite image of the supercell progressing over broader area of Zagreb. Source: EUMETSAT (for the overall coordinates and positioning, see Fig. 1 and 2). *b*) EUMETSAT European HRV RGB (High Resolution Visible Red, Green, and Blue) timeline satellite images of the supercell progressing from its origin area to the exit from Croatia toward east. The images are 2 h apart, with the first at 07 UTC and the last at 21 UTC.

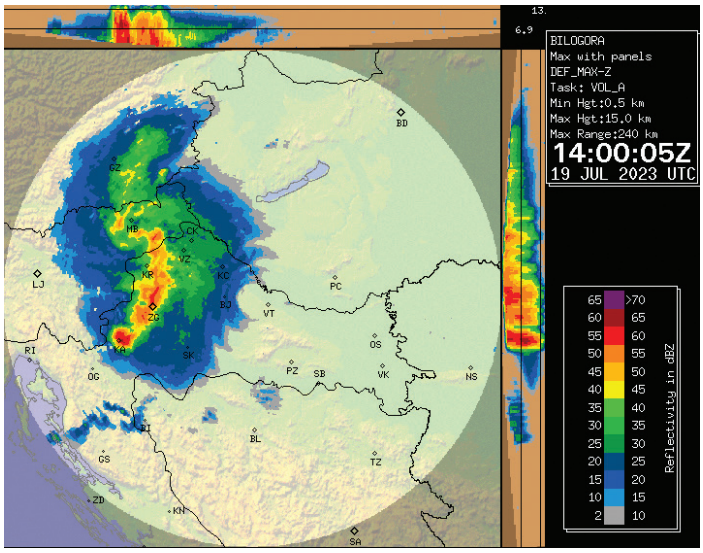

Figure 6. Radar reflectivity in dBZ of the supercell system at 14 UTC, 19 July 2023, as measured by the Bilogora radar DHMZ, (elevation 259 m ASL) located about 15 km WNW from the town of Virovitica, VT, and cca 70 km ENE from the city of Zagreb air distance.

log-P diagrams were employed to better understand the vertical structure of the atmosphere, which is crucial for determining the amount of SBCAPE and SB-CIN, their vertical distribution, temperature, dew point gradients, and wind shear data in the lowest 2 km AGL. Meteograms provided an additional picture of the temporal development of the weather situation, indicating changes in various meteorological parameters in time.

3.5.1. Precipitation and radar reflectivity

The precipitation, Fig. 7, derived from the simulation exhibits reasonable agreement with the radar imagery, Fig. 6, affirming the model's capability to replicate this event with adequate accuracy. Interestingly, in the precipitation simulation during the passage of the supercell over Zagreb, Fig. 7, the separation of the supercell into three cores is visible. Over the next hour, the southern core strengthens, the northern one dissipates, in accordance with the typical behaviour of supercell (*e.g.*, Holton, 1992), but it is currently unclear whether the central core merges with the southern one or it also dissipates.

Radar reflectivity image derived from the WRF-ARW simulation, Fig. 8, shows bended convective storm structure indicating so called bow echo (Johns, 1993). Bow echo convective storm structure is associated with intense damaging winds and/or downbursts or microbursts indicating that this could be a derecho event as well (Johns and Hirt, 1987).

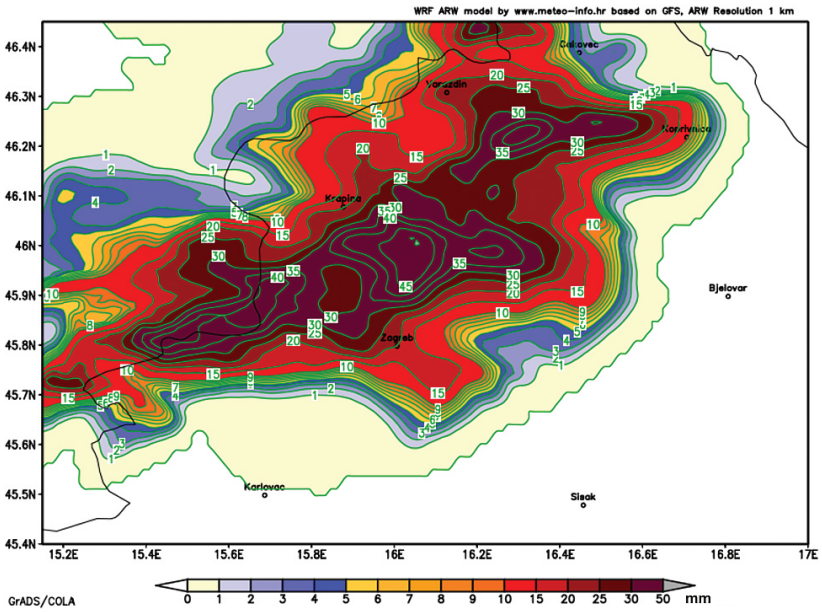

Figure 7. WRF-ARW simulation of the 30 min precipitation field, domain d03, from 14:30 to 15:00 UTC, 19 July 2023. The city of Zagreb and surrounding towns are indicated. Note the vigorous intensity of the precipitation locally reaching over 40 mm in 30 min (the colorbars scale is not linear).

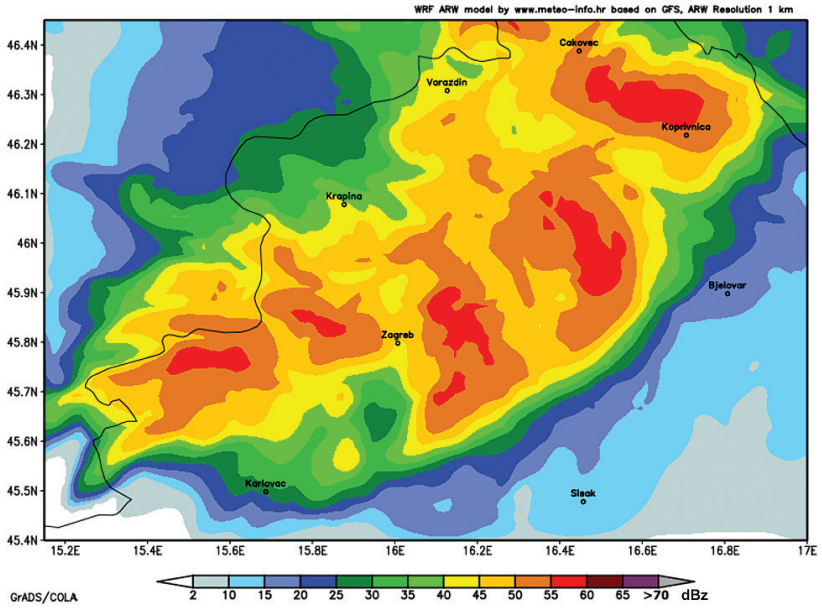

Figure 8. WRF-ARW simulation of radar reflectivity field (dBZ), domain d03, at 15 UTC 19 July.

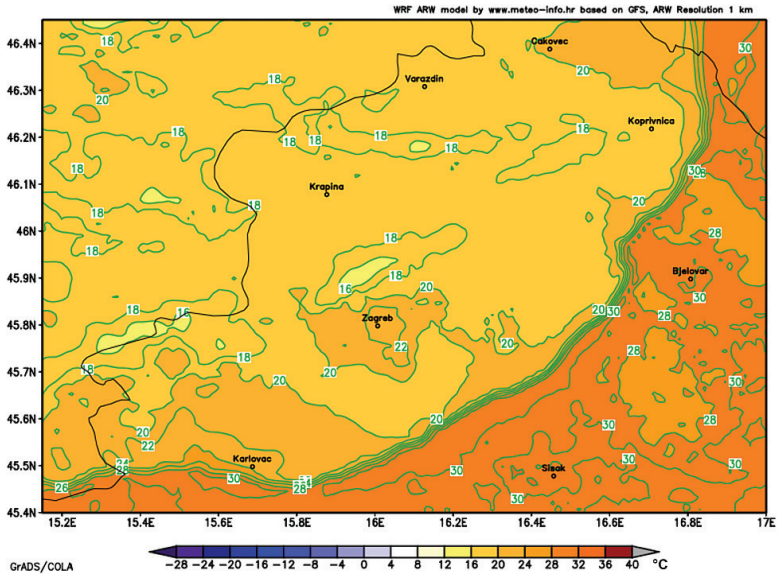

Figure 9. WRF-ARW simulation of temperature at 2m at 15 UTC 19 July 2023. The city of Zagreb and surrounding towns are indicated as well as the Croatian-Slovenian border and Croatian-Hungarian border ((left and upper right, respectively). Note that the thickness of the rapidly propagating mesoscale front is only a few km, *i.e.*, as fine as the innermost model grid might resolve it. Horizontal temperature gradient through mesofront was 8-10 K/km.

3.5.2. Temperature field

The 2 m temperature field, shown in Fig. 9, reveals the propagation of the associated mesoscale cold front, preceded by the warm air with temperatures ranging from 30 to 32 °C. Within cold air, called cold pool, behind the mesoscale front, the simulated temperatures were substantially lower with values between 18 and 20 °C. Cold pool is a cold pocket of dense air that forms when rain evaporates during intense precipitation *e.g.* underneath a thunderstorm cloud or a precipitating shallow cloud. Typically, cold pools spread at 10 m/s and last 2–3 h. Cold pools are ubiquitous both over land and ocean. The width of the frontal zone was only a few kilometres. In less than 1 h, the modelled front progressed from Zagreb to the town of Sisak that is 60 km away toward southeast. Comparing the mesoscale cold front baroclinic boundary of the supercell on 30th August 2003 in Stiperski (2005) with the analysed baroclinic boundary of the supercell on 19th July 2023, a similar pattern can be observed.

3.5.3. Wind and pressure

The modelled wind fields at 10 and 80 m AGL show the rapid propagation of cold air associated with the system's downdraft and the gust front imbedded into mesofront. Simulated wind speeds at 10 m and 80 m AGL, Figs. 10 and 11,

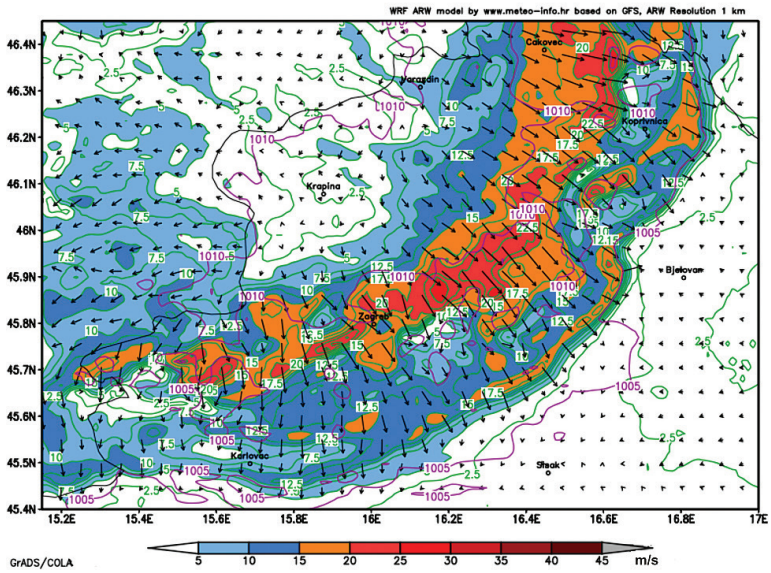

Figure 10. The wind field at 10 m above ground level over north-western Croatia on 19 July 2023 at 15 UTC, as simulated by the WRF ARW model with a 1 km grid spacing. The colours indicate wind speed in m/s, with the highest values in red areas, while arrows represent wind direction. Note the strong winds concentrated in the southern part of the region, with speeds exceeding 25 m/s, suggesting intense surface-level wind dynamics associated with the passing supercell system.

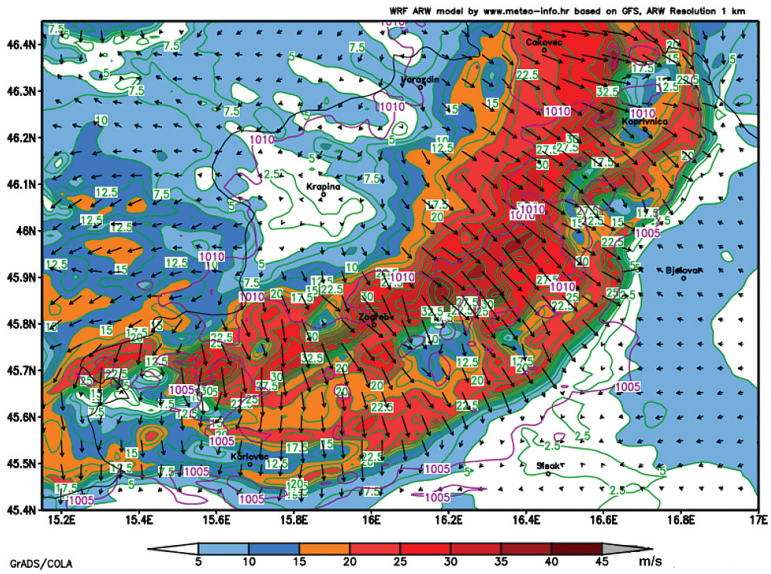

Figure 11. Same as Fig. 10, but at 80 m above ground level.

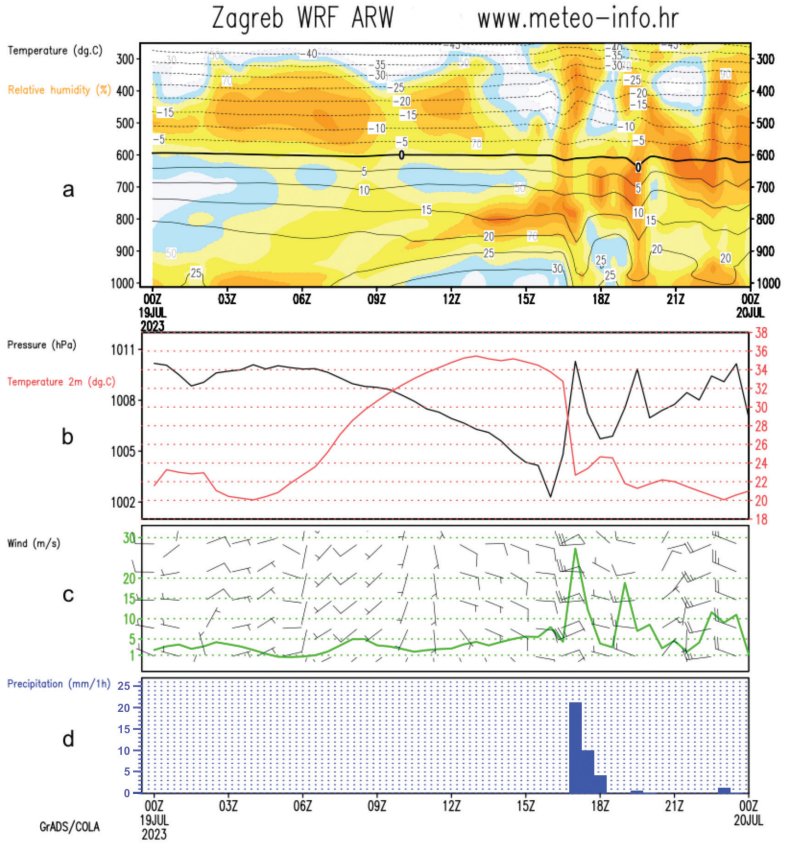

Figure 12. Meteogram for Zagreb (Lat: 45.73° N, Lon: 15.89° E) on 19 July 2023, derived from the WRF-ARW simulation, detailing the atmospheric conditions associated with the supercell storm. Panel (*a*) illustrates the vertical profile of relative humidity and temperature. Panel (*b*) presents surface pressure and 2-meter air temperature. Panel (*c*) details wind speed and direction at different altitudes. Panel (*d*) presents precipitation rates.

reach up to 35 and 45 m/s, respectively. The wind field exhibits similar pattern of speeds and directions at all calculated levels from the ground up to 800 hPa level. The mesoscale front is again very narrow, and it moves rapidly. Almost needless to say, this is one of the advantages of fine scale numerical simulations where all the main meteorological fields are mutually interrelated in a dynamically consistent way.

Simulated meteogram, Fig. 12, shows several variables. In Fig. 12a relative humidity (RH) and temperature are presented. RH field shows that the supercell top exceeds 350 hPa altitudes. Temperature curves in Fig. 12a shows short temperature drops below 850 hPa due to evaporation of the precipitation, as well as

melting of snow/hail into rain which absorbs the latent heat from the air. Simulated surface pressure, shown in Fig. 12b, displays an unusual shape, yet typical for supercell (Klemp, 1987). From the morning until the onset of the event, the pressure steadily decreases from the initial 1,010 hPa to 1,004 hPa. Just before the passage of the supercell, the pressure sharply drops to 1,002 hPa. Subsequently, in about 1 h, it rises to 1,010 hPa, then it rapidly drops again to 1,006 hPa continuing to oscillate. The pressure curve in the simulated meteogram resembles damped oscillations. With the onset of a new storm, just before the midnight on the 19 July 2023, the pressure curve in Fig. 12b decreases again. The measured pressure data from Maksimir station, Zagreb east, not presented here, show oscillation with lower amplitudes. Fig. 12c displays wind speed and direction at different altitudes, highlighting a significant increase in wind speed up to 30 m/s as the storm intensifies around 18Z. Fig. 12d displays precipitation rates, showing a burst of heavy rainfall reaching up to 25 mm/h, which coincides with the peak of the storm in Zagreb (Lat: 45.73° N, Lon: 15.89° E), underscoring the supercell's severe impact.

3.5.4. Skew-T log-P analysis

The skew-T log-P diagrams, Fig. 13, obtained through the numerical simulation aligns quite well with those obtained from the radiosondes shown in Fig. 4.

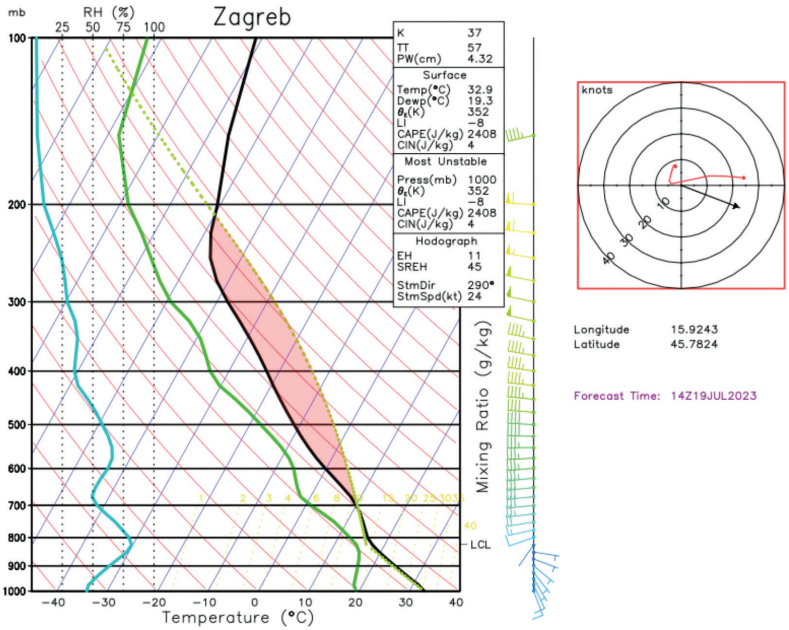

Figure 13. The Zagreb Skew-T log-P and hodograph for 19 July 2023, derived from the WRF-ARW. Red area represents CAPE while blue one presents CIN. Velocity converter: 1 knot ≈ 0.5 m/s.

This diagram shows a strong wind shear between 850 and 800 hPa corresponding to altitudes of about 1,500–2,000 m. Between 350 and 250 hPa, a strong jet stream is present. SBCAPE values were between 2,000 and 2,400 J/kg, while lifted index was –8 °C and SBCIN value only 21 J/kg. The presented highly curved initial part of the hodograph in Fig. 13, the right side, reveals strong directional shear in the lower part of the troposphere, while elongated path towards upper layers indicates strong wind speed shear in the middle troposphere. This shape corresponds to a typical wind hodograph associated with supercell conditions (Weisman and Klemp, 1986).

The combination of Energy Helicity Index (EH) value of 11 and Storm Relative Helicity (SREH) value of 45 m^2/s^2 suggests favourable conditions for the development of tornadoes or other severe weather phenomena. Helicity is a significant and important measure of coherent structures in flows (*e.g.*, Lesieur, 1997; Grisogono et al., 2024). There are two possible interpretations of this situation:

1. High energy and moderate rotation: An EH value of 11 indicates high levels of atmospheric instability, meaning there is an abundance of energy that supports intense vertical development of storms. On the other hand, SREH of 45 m2/s2 suggests the presence of rotational characteristics in the troposphere.

2. Increased tornado risk: The combination of high EH value and moderate SREH value enhances the likelihood of tornadogenesis. High energy suggests there is enough potential energy, relating to CAPE, for the intense development of storms, while rotational characteristics, relating to helicity, suggest the presence of vorticity that could support tornado formation.

In any case, this combination of parameters suggests a high risk of severe weather phenomena, particularly tornadoes, etc.

3.5.5. Vertical cross sections

To analyse the structure and dynamics of the convective storm that developed on July 19, 2023, we performed a numerical simulation using the Weather Research and Forecasting (WRF) model with the Advanced Research WRF (ARW) core. The simulation was configured with high spatial and temporal resolution, allowing for a detailed examination of the storm's evolution.

Figure 14 presents the vertical distribution of radar reflectivity (dBZ) at 16:30 UTC along a transect following the 16.20° meridian, from 45.70° to 46.60° latitude. The highest reflectivity values, exceeding 55 dBZ, are concentrated between 2 and 10 km in altitude, indicating intense convective activity and the presence of strong updrafts, as stated above as a likely possibility. The reflectivity structure suggests the development of a deep convective core, with precipitation processes extending above the freezing level (~5 km). High reflectivity values above 10 km suggest potential hail formation and the influence of strong vertical motions.

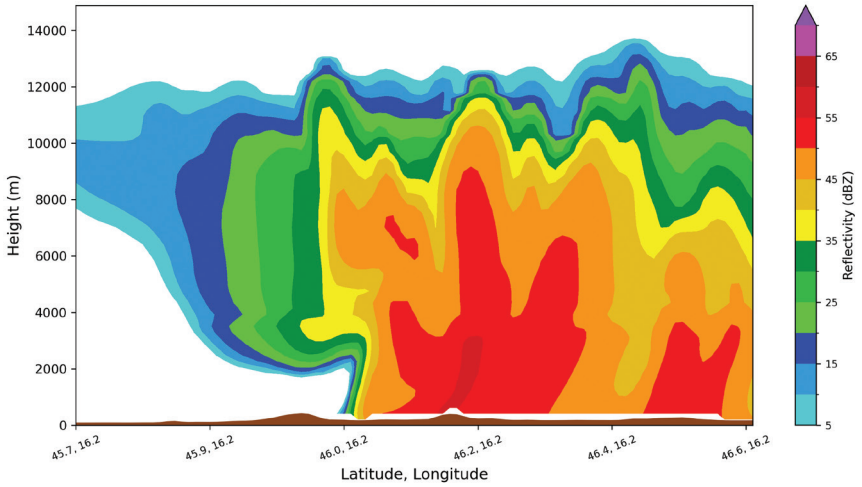

Figure 14. Vertical distribution of radar reflectivity (dBZ) at 16:30 UTC. The transect goes along the 16.20 meridian and from 45.70 to 46.60 latitude.

Figure 15 presents the vertical temperature distribution (°C) along the same transects. A well-defined temperature gradient is evident, with warmer air in the lower troposphere and progressive cooling with height. The convective system induces local perturbations in the thermal structure, leading to cooling near strong updrafts. These regions correspond to areas where latent heat release and adiabatic cooling occur, thus further sustaining deep convection.

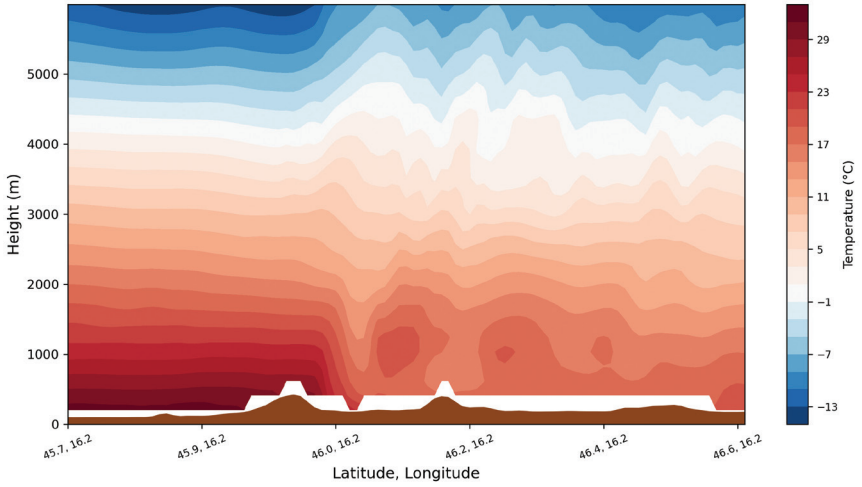

Figure 15. Temperature vertical distribution (°C) at 16:30 UTC along the same cross-section.

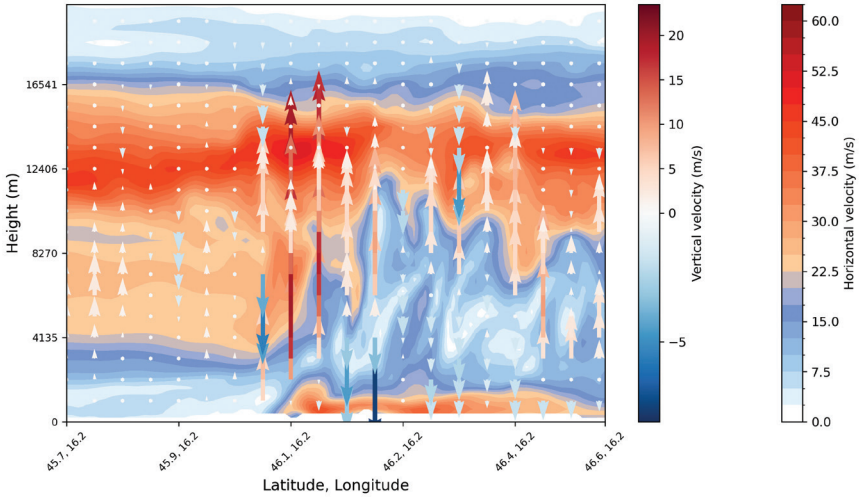

Figure 16. Distribution of wind speed (m/s), overlaid with vertical velocity vectors along the same transect at 16:30 UTC. The colour bar on the right represents horizontal wind speed, while the colour bar on the left represents vertical wind speed.

Figure 16 presents the vertical cross-section of horizontal wind speed (m/s), overlaid with vertical velocity vectors along the same transect. Strong updrafts exceeding 20 m/s are evident within the storm's core, facilitating and being one of the keys of mesoscale dynamics and the development of deep convection. Downdrafts are also present, particularly along the storm's periphery, contributing to outflow dynamics and cold pool formation. The colour shading represents horizontal wind speed, with the highest values (~40–50 m/s) observed at upper levels, highlighting the influence of the jet stream and storm-relative inflow.

These vertical cross-sections confirm the presence of a well-organized deep convective system, characterized by intense reflectivity cores, strong updrafts, and significant thermal gradients. The interaction of dynamical and thermodynamical processes within the storm aligns with the mechanisms responsible for severe convective weather events.

4. Discussion

Predicting the occurrence and development of thunderstorms poses a significant challenge in operational meteorology and is associated with substantial economic losses. The true extent of the damages might never be determined. Every analysis of such extreme events contributes to a better understanding and eventually more accurate forecasting in future. Timely information to the public and relevant state services is an immense responsibility for national meteoro-

logical services. In this preliminary study, main aspects of a supercell storm in Croatia on 19 July 2023 are assessed.

In the case of the analysed event, the main synoptic-scale mechanism for the forcing of the initiation and development of the supercell system was a strong wind shear at altitudes between 1,500 and 2,000 m (850–800 hPa) and the presence of a strong zonal jet stream over the central Europe. The main mesoscale feature was the formation of a baroclinic boundary over the Po River valley in Italy early in the morning. After the initiation of the convective cloud system, the baroclinic boundary rapidly moved towards Slovenia, transforming the system along the way into a supercell. The baroclinic boundary was approximately 350-400 km long and had a crescent shape. The convective storm system lasted for about 10 h (EUMETSAT) and progressed about 1000 km in an almost straight line, so it satisfies the conditions to be classified even as a derecho.

The Po River valley provides ideal conditions for the development of severe convective storms (*e.g.*, Buzzi et al., 1992; Cacciamani et al., 1995), including supercells, all due to a combination of synoptic, mesoscale, and orographic factors. The valley's enclosed geography, bordered by the Alps to the north and the Apennines to the south, enhances low-level moisture convergence and facilitates the accumulation of warm, humid air. Additionally, the valley frequently experiences strong wind shear, particularly when southerly low-level winds from the Mediterranean interact with westerly or north-westerly upper-level flow. This configuration promotes storm organization and rotation, essential for supercell formation. Moreover, mesoscale boundaries, such as sea breeze fronts and outflow boundaries from previous convection, often act as triggers for deep convection (Fu et al., 2022). The combination of high instability and strong vertical wind shear makes the Po Valley a hotspot for severe convective storms in southern Europe. Under the influence of global planetary circulation and overall synoptic extratropical airflows, convective storm systems tend to move eastward; hence, they generally support the related long-lived storms to reach Slovenia, Croatia and further east.

The analysed case clearly shows the damage risk these storms pose to the area, thus justifying the need for more detailed research and understanding of such events. All available forecasting materials indicated a high probability of a devastating storm, highlighting the need for greater attention to the analysis of supercells. This is especially important for determining which forecasting parameters clearly and unequivocally indicate the possibility of the formation of supercells.

To the crucial question: how predictable such events are - what is the reliability and how far in advance can they be predicted? It is currently not possible to provide a completely precise answer (*e.g.*, Gregorič et al., 2003). This study indicates how likely is the occurrence of an intense storm; strong wind shear suggested a high probability of convective storm to become of a supercell type, answering the first part of the question positively. However, the answer to the

second part of the question – how far in advance could such event be predicted with a satisfactory probability of occurrence – it remains open and will require further research in the form of numerical simulations. To put it in another way, the mechanism for deep convection and the main ingredients are known (Klemp, 1987), but the triggers in specific situations are not.

5. Conclusion

The 19 July 2023 supercell storm over Croatia serves as a significant example of the destructive potential of such severe convective systems. Originating in Italy, the storm travelled over 1,000 km, impacting multiple countries and causing extensive damage, fatalities, and a record-breaking hail event in Croatia. The analysis highlights the critical role of synoptic and mesoscale conditions, particularly the strong vertical wind shear and baroclinic boundary layer that fostered the storm's intensity and longevity.

This study underscores the need for enhanced forecasting models and greater understanding of supercells in this region. The findings emphasize that, while predicting such events with precision remains challenging, the identification of key parameters, such as wind shear and atmospheric instability, can significantly improve the accuracy of early warnings and preparedness efforts. This case study not only contributes to the limited research on supercells in Croatia but also provides valuable insights that can inform future studies and support meteorological advancements in the region.

Acknowledgements – This study was partially funded by the Croatian science foundation project C3PO (HRZZ-IP-2022-10-9139). The Croatian Weather Service is thanked for providing radar images and notes in the Hail Defence Service diary.

References

Alberoni, P. P., Nanni, S., Crespi, M. and Monai, M. (1996): The supercell thunderstorm on 8 June 1990: Mesoscale analysis and radar observations, *Meteorol. Atmos. Phys.*, **58**, 123–138, https://doi.org/10.1007/BF01027560.

Bunkers, M. J., Hjelmfelt, M. R. and Smith, L. P. (2006): An observational examination of long-lived supercells. Part I: Characteristics, evolution, and demise, *B. Am. Meteorol. Soc.,* **21**(5), 673–688, https://doi.org/10.1175/WAF949.1.

Buzzi, A. and Alberoni, P. P. (1992): Analysis and numerical modelling of a frontal passage associated with thunderstorm development over the Po valley and the Adriatic Sea, *Meteorol. Atmos. Phys*., **48**, 205–224, https://doi.org/10.1007/BF01029569.

Chen, S.-H. and Sun, W.-Y. (2002): A one-dimensional time dependent cloud model, *J. Meteorol. Soc. Jpn*., **80**(1), 99–118, https://doi.org/10.2151/jmsj.80.99.

Cacciamani, C., Battaglia, F., Patruno, P., Pomi, L., Selvini, A. and Tibaldi, S. (1995): A climatological study of thunderstorm activity in the Po Valley, *Theor. Appl. Climatol.*, **50**, 185–203, https://doi.org/10.1007/BF00866116.

Davolio, S., Mastrangelo, D., Miglietta, M. M., Drofa, O., Buzzi, A. and Malguzzi, P. (2009): High resolution simulations of a flash flood near Venice, *Nat. Hazards Earth Syst. Sci.*, **9**, 1671–1678, https://doi.org/10.5194/nhess-9-1671-2009.

Ducrocq, V., Braud, I., Davolio, S., Ferretti, R., Flamant, C., Jansa, A., Kalthoff, N., Richard, E., Taupier-Letage, I., Ayral, P. A., Belamari, S., Berne, A., Borga, M., Boudevillain, B., Bock, O., Boichard, J. L., Bouin, M. N., Bousquet, O., Bouvier, C. and Tamayo, J. (2014): HyMeX-SOP1: The field campaign dedicated to heavy precipitation and flash flooding in the Northwestern Mediterranean, *B. Am. Meteorol. Soc.*, **95**(7), 1083–1100, https://doi.org/10.1175/BAMS-D-12-00244.1.

EUMETSAT (n.d.) https://view.eumetsat.int/productviewer?v=defaultEUMETSAT (2021): Algorithm Theoretical Basis Documents for Convection (ATBD). Retrieved from https://www.nwcsaf.org/Downloads/GEO/2021/Documents/Scientific_Docs/NWC-CDOP3-GEO-MF-PI-SCI-ATBD-Convection_v1.0.1.pdf.

EUMETSAT (2021): Product User Manual for Convection (UM). Retrieved from https://www.nwcsaf.org/Downloads/GEO/2021/Documents/Scientific_Docs/NWC-CDOP3-GEO-MF-PI-SCI-UM-Convection_v2.0.1.pdf.

Feldmann, M., Rotunno, R., Germann, U. and Berne, A. (2004): Supercell thunderstorms in complex topography—How mountain valleys with lakes can increase occurrence frequency, *Mon. Weather Rev.*, **152**, 471–489, https://doi.org/10.1175/MWR-D-22-0350.1.

Fu, S., Rotunno, R. and Xue, H. (2022): Convective updrafts near sea-breeze fronts, *Atmos. Chem. Phys.*, **22**, 7727–7738, https://doi.org/10.5194/acp-22-7727-2022.

Gatzen, C. (2004): A derecho in Europe: Berlin, 10 July 2002, *Weather Forecast.*, **19**(3), 639–645, https://doi.org/10.1175/1520-0434(2004)019<0639:ADIEBJ>2.0.CO;2.

Giovannini, L., Davolio, S., Zaramella, M., Zardi, D. and Borga, M. (2021): Multi-model convection-resolving simulations of the October 2018 Vaia storm over Northeastern Italy, *Atmos. Res.*, **253**, 105455, https://doi.org/10.1016/j.atmosres.2021.105455.

Gospodinov, I., Dimitrova, T., Bocheva, L., Simeonov, P. and Dimitrov, R. (2015): Derecho-like event in Bulgaria on 20 July 2011, *Atmos. Res.*, **158–159**, 254–273, https://doi.org/10.1016/j.atmosres.2014.05.009.

Gregorič, G., Iršič, M. and Zgonc, T. (2003): Survey of convective supercell in Slovenia with validation of operational model forecasts, *Atmos. Res.*, **67–68**, 261–271, https://doi.org/10.1016/S0169-8095(03)00055-3

Grisogono, B., Večenaj, Ž. and Belušić, D. (2024): Uvod u mezoskalnu meteorologiju i atmosfersku turbulenciju (Lectures in Dynamic meteorology, internal scripts), 186 pp (in Croatian), https://www.croris.hr/crosbi/publikacija/rad-ostalo/760823.

Holton, J. R. (1992 or 2004): *An Introduction to Dynamic Meteorology*, Academic Press 3rd edition (or 4th edition), San Diego, USA, 511 pp.

Huang, M., Mielikainen, J., Huang, B., Chen, H., Huang, H.-L. A. and Goldberg, M. D. (2015): Development of efficient GPU parallelization of WRF Yonsei University planetary boundary layer scheme, *Geosci. Model Dev.,* **8**(9), 2977–2990, https://doi.org/10.5194/gmd-8-2977-2015.

Jiménez, P. A., Dudhia, J., González-Rouco, J. F., Navarro, J., Montávez, J. P. and García-Bustamante, E. (2012): A revised scheme for the WRF surface layer formulation, *Mon. Weather Rev.*, **140**(3), 898–918, https://doi.org/10.1175/MWR-D-11-00056.1.

Johns, R. H, (1993): Meteorological Conditions Associated with Bow Echo Development in Convective Storms, *Weather Forecast.*, **8**(2), 294–299, https://doi.org/10.1175/1520-0434(1993)008<0294:MCAWBE>2.0.CO;2.

Johns, R. H. and Hirt, W. D. (1987): Widespread convectively induced windstorms, *Weather Forecast.*, **2**, 32–49, https://doi.org/10.1175/1520-0434(1987)002<0032:DWCIW>2.0.CO;2.

Klemp, J. B. (1987): Dynamics of tornadic thunderstorms, *Annu. Rev. Fluid Mech.*, **19**, 369–402, https://doi.org/10.1146/annurev.fl.19.010187.002101.

Kwon, Y. C. and Hong, S. (2017): A mass-flux cumulus parameterization scheme across gray-zone resolutions, *Mon. Weather Rev.*, **145**(2), 583–598, https://doi.org/10.1175/MWR-D-16-0034.1.

Lesieur, M. (1997): *Turbulence in fluids*. Kluwer (3rd edition), Dordrecht, the Netherlands, 515 pp.

Orf, L., Wilhelmson, R., Lee, B., Finley, C. and Houston, A. (2017): Evolution of a long-track violent tornado within a simulated supercell, *B. Am. Meteorol. Soc.*, **98**(1), 45–68, https://doi.org/10.1175/BAMS-D-15-00073.1.

Pacey, G. P., Schultz, D. M. and Garcia-Carreras, L. L. (2021): Severe convective windstorms in Europe: Climatology, preconvective environments, and convective mode, *Weather Forecast.*, **36**, 237–252, https://doi.org/10.1175/WAF-D-20-0075.1.

Pilguj, N., Taszarek, M., Kryza, M. and Brooks, H. E. (2022): Reconstruction of violent tornado environments in Europe: High-resolution dynamical downscaling of ERA5, *Geophys. Res. Lett.*, **49**(11), https://doi.org/10.1029/2022GL098242.

Púčik, T., Groenemeijer, P., Rädler, A. T., Tijssen, L., Nikulin, G., Prein, A. F., van Meijgaard, E., Fealy, R., Jacob, D. and Teichmann, C. (2017): Future changes in European severe convection environments in a regional climate model ensemble, *J. Clim.*, **30**(17), 6771–6794, https://doi.org/10.1175/JCLI-D-16-0777.1.

Ricchi, A., Sangelantoni, L., Redaelli, G. and Ferretti, R. (2020): Investigating triggering mechanisms for the large hailstorm event of July 10th, 2019 on the Adriatic Sea, in: *EGU General Assembly Conference Abstracts*, p. 17847.

Ricchi, A., Sangelantoni, L., Redaelli, G., Mazzarella, V., Montopoli, M., Miglietta, M. M., Tiesi, A., Mazzà, S., Rotunno, R. and Ferretti, R. (2023): Impact of the SST and topography on the development of a large-hail storm event, on the Adriatic Sea, *Atmos. Res.*, **296**, 107078, https://doi.org/10.1016/J.ATMOSRES.2023.107078-

Sano, T. and Tsuboki, K. (2006): Structure and evolution of a cumulonimbus cloud developed over a mountain slope with the arrival of sea breeze in summer, *J. Meteorol. Soc. Jpn.*, **84**(4), 613–640, https://doi.org/10.2151/jmsj.84.613.

Skamarock, W. C., Klemp, J. B., Dudhia, J., Gill, D. O., Liu, Z., Berner, J. and Huang, X.-Y. (2021): A description of the advanced research WRF model version 4.3 (No. NCAR/TN-556+STR), https://doi.org/10.5065/1dfh-6p97.

Smith, G. M. and Lin, Y.-L. (2016). The effects of orographic geometry on supercell thunderstorms, *arXiv:1603.00579 [physics.ao-ph]*, https://doi.org/10.48550/arXiv.1603.00579.

Smith, G. M., Lin, Y.-L. and Rastigejev, Y. (2016a): Orographic effects on supercell: Development, structure, intensity, and tracking, *arXiv:1603.00539 [physics.ao-ph]*, https://doi.org/10.48550/arXiv.1603.00539.

Squitieri, B. J., Wade, A. R. and Jirak, I. L. (2023): A historical overview on the science of derechos. Part I: Identification, climatology, and societal impacts, *B. Am. Meteorol. Soc.*, **104**(10), E1709-E1733, https://doi.org/10.1175/BAMS-D-22-0217.1.

Stiperski, I. (2005): The causes of supercell development with tornadogenesis on 30th August 2003 – A casestudy, *Geofizika*, **22**, 83–104, http://geofizika-journal.gfz.hr/vol_22/stiperski.pdf.

Strelec Mahović, N. (2007): Numerical simulation of severe convective phenomena over Croatian and Hungarian territory, *Atmos. Res.* **83**(2–4), 121–131, https://doi.org/10.1016/j.atmosres.2005.09.011.

Strelec Mahović, N., Plačko-Vršnak, D. and Mazzocco Drvar, D. (2014): Sinoptička i mezoskalna analiza tučonosnih oluja iznad Hrvatske 22. i 23. lipnja 2007., *Hrvatski meteorološki časopis – Croatian Meteorologival Journal*, **47**, 57–67 (in Croatian), https://hrcak.srce.hr/115913.

Taszarek, M., Allen, J. T., Brooks, H. E., Pilguj, N. and Czernecki, B. (2021): Differing trends in United States and European severe thunderstorm environments in a warming climate, *B. Am. Meteorol. Soc.*, **102**(2), E296-E322, https://doi.org/10.1175/BAMS-D-20-0004.1.

Taszarek, M., Pilguj, N., Orlikowski, J., Surowiecki, A., Walczakiewicz, S., Pilorz, W., Piasecki, K., Pajurek, Ł. and Półrolniczak, M. (2019a): Derecho evolving from a mesocyclone—A study of 11 August 2017 severe weather outbreak in Poland: Event analysis and high-resolution simulation, *Mon. Weather Rev.*, **147**(6), 2283–2306, https://doi.org/10.1175/MWR-D-18-0330.1.

Taszarek, M., Allen, J., Púčik, T., Groenemeijer, P., Czernecki, B., Kolendowicz, L., Lagouvardos, K., Kotroni, K. and Schulz, W. (2019b): A climatology of thunderstorms across Europe from a synthesis of multiple data sources, *J. Clim.*, **32**(6), 1813–1837, https://doi.org/10.1175/JCLI-D-18-0372.1.

Tewari, M., Chen, F., Wang, W., Dudhia, J., LeMone, M. A., Mitchell, K., Ek, M., Gayno, G., Wegiel, J. and Cuenca, R. H. (2004): Implementation and verification of the unified NOAH land surface model in the WRF model, *20th Conference on Weather Analysis and Forecasting / 16th Conference*

on Numerical Weather Prediction,
https://www2.mmm.ucar.edu/wrf/users/physics/phys_refs/LAND_SURFACE/noah.pdf

Tiesi, A., Mazza', S., Conte, D., Ricchi, A., Baldini, L., Montopoli, M., Picciotti, E., Vulpiani, G., Ferretti, R., Miglietta, M.M., (2022): Numerical simulation of a giant-hail-bearing Mediterranean supercell in the Adriatic Sea, *Atmosphere*, **13**(8), 1219, https://doi.org/10.3390/ATMOS13081219.

Weisman, M. L., Evans, C. and Bosart. L, (2013): The 8 May 2009 Superderecho: Analysis of a Real-Time Explicit Convective Forecast, *Weather Forecast.*, **28**, 863–892,
https://doi.org/10.1175/WAF-D-12-00023.1.

Weisman, M.L. and Klemp, J. B. (1986): Characteristics of isolated convective storms, in: *Mesoscale meteorology and forecasting*, edited by Ray, P. S., *AMS*, Boston, MA,
https://doi.org/10.1007/978-1-935704-20-1_15.

Zheng, Y., Alapaty, K., Herwehe, J. A., Del Genio, A. D. and Niyogi, D. (2016): Improving high-resolution weather forecasts using the weather research and forecasting (WRF) model with an updated Kain–Fritsch scheme, *Mon. Weather Rev.*, **144**(3), 833–860,
https://doi.org/10.1175/MWR-D-15-0005.1.

SAŽETAK

Kratka analiza superćelijske oluje u Hrvatskoj 19. srpnja 2023.

Nebojša Subanović, Ivan Toman, Patrik Jureša i Branko Grisogono

Superćelijski kumulonimbusi su moćni i dugotrajni konvektivni sustavi koji se mogu formirati unutar nestabilne zračne mase u povoljnim dinamičkim uvjetima. Ovakve žestoke oluje karakteriziraju se jednim ili više rotirajućih uspona zraka podržanih vertikalnim smicanjem vjetra u okolini. Razornost ovih sustava obično se odražava u obilnoj kiši i pljuskovima, velikoj tuči, orkanskim udarima vjetra i ponekad događajima poput „derechoa“ ili tornada.

Tijekom 19. srpnja 2023, u Hrvatskoj se pojavila superćelija, koja je pogodila i glavni grad Zagreb. Nastala je u zapadnom dijelu doline rijeke Po u Italiji, prošla kroz Sloveniju i Hrvatsku te se naposljetku raspršila preko Srbije. Na svom putu super-oluja je prešla oko 1000 km i trajala je oko 10 h, uzrokujući ljudske žrtve i velike štete na imovini.

U ovom radu analiziraju se i raspravljaju sinoptički i posebice mezoskalni uvjeti koji su doveli do formiranja ovog sustava. Korišteni materijali uključuju podatke s postaja, sinoptičke karte, radio sondažna mjerenja gornje atmosfere, radarske i satelitske slike, kao i simulaciju modela WRF koja je provedena za ovaj scenarij. Ovo istraživanje treba pomoći boljem razumijevanju takvih fenomena i njihovog destruktivnog potencijala iznad šireg područja Hrvatske te doprinosi relativno oskudnim istraživanjima ovakvog tipa vremena u ovom dijelu svijeta.

Ključne riječi: mezoskalna fronta, žestoke konvektivne oluje, „derecho“, „bow echo“

Corresponding author's address: Nebojša Subanović, Power Net simple Ltd., Poljana Z. Mikine 46, 10000 Zagreb,; tel: +385 91 3832 183; e-mail: nebojsa.subanovic@meteo-info.hr